Electrocatalysis

Deutsche Ausgabe: DOI: 10.1002/ange.201503917
Internationale Ausgabe: DOI: 10.1002/anie.201503917

Irrelevance of Carbon Monoxide Poisoning in the Methanol Oxidation Reaction on a PtRu Electrocatalyst**

*De-Jun Chen and YuYe J. Tong**

Abstract: *Based on detailed in situ attenuated total-reflection–surface-enhanced IR reflection absorption spectroscopy (ATR-SEIRAS) studies of the methanol oxidation reaction (MOR) on Ru/Pt thin film and commercial Johnson–Matthey PtRu/C, a revised MOR enhancement mechanism is proposed in which CO on Pt sites is irrelevant but instead Pt-Ru boundary sites catalyze the oxygen insertion reaction that leads to the formation of formate and enhances the direct reaction pathway.*

The methanol (MeOH) oxidation reaction (MOR) is not only an important model reaction in oxidation of small organic molecules[1] but also a promising fuel for the so-called methanol economy in general[2] and direct MeOH fuel cells (DMFCs) in particular.[3] For MOR on Pt, it is generally accepted, notwithstanding the debates,[4] that the reaction can have parallel duel paths: indirect CO poisoning and direct formate paths.[5] However, a pure Pt surface is heavily poisoned by CO within the potential range that is relevant to economically viable DMFC applications, which has to be < 0.6 V (vs. reversible hydrogen electrode/RHE to which all potentials herein will be referred) because the cell potential approaches zero at 0.6 V.[6] In this regard, PtRu is still among the best performing CO-poisoning-tolerant electrocatalysts for MOR.[7] The conventional rationalization of such superior catalytic performance is the Watanabe–Motoo (W-M) bifunctional mechanism proposed about four decades ago[8] in which the more oxophilic Ru is thought to provide oxygen-containing species that enable the oxidation of poisonous CO on the adjacent Pt at a much lower overpotential. This can be expressed as:

$$\mathrm{Pt{-}CO + HO{-}Ru \rightarrow Pt^{*} + Ru^{*} + CO_2 + H^{+} + e^{-}} \quad (1)$$

where Pt* and Ru* stand for the freed Pt and Ru sites.[9]

While the W-M bifunctional mechanism as stated in Reaction (1) has seemly been supported by strong circumstantial evidence[10] and is widely accepted, there is still a lack of direct molecular-level evidence to prove or disprove it. On the other hand it was observed in early studies of MOR on PtRu[11] that, notwithstanding strong CO_2 production at about 0.5 V, the amount of adsorbed CO did not decrease, which is in an apparent contradiction to Reaction (1) but was argued then to be caused by a steady-state process in which the rate of adsorbing CO equaled to its oxidation. In a recent study of the chemistry of PtRu activation,[12] we have observed the same persistence of the adsorbed CO while MOR was actively operational, which prompted us to revisit the W-M bifunctional mechanism. We carried out detailed in situ attenuated total-reflection–surface-enhanced IR reflection absorption spectroscopy (ATR-SEIRAS)[13] investigations of MOR on two morphologically different PtRu samples, Ru-decorated Pt thin film (Ru/Pt) and commercial (Johnson-Matthey) carbon-supported PtRu (1:1, 60 wt.%, and 3.1 nm average size) electrocatalyst (PtRu/C). We also focused only on the MOR mechanism at low overpotential (< 0.5 V) as the maximum power output of a DMFC is usually reached below 0.5 V (Supporting Information, Figure S1).[6] Moreover, we augmented the in situ ATR-SEIRAS by coupling it with flow-cell and isotope-labeling operations. We discovered that the experimentally observed enhancement in MOR activity on both the Ru/Pt and J-M PtRu/C had little to do with Reaction (1) but with enhancing the direct reaction pathway in which formate is expected to be a reaction intermediate.[5c,d] This leads us to propose a new revised bifunctional mechanism that we present herein.

For our in situ ATR-SEIRAS studies, the Ru/Pt was made as follows. An ultrathin (ca. 90 nm) Pt film (Figure S2) was deposited onto a triangular Si prism that was used as the IR window. A monolayer Ru was then electrodeposited onto the pre-formed Pt thin film in the assembled in situ ATR-SEIRAS cell (Figure S3). The most activated Ru/Pt (act-Ru/Pt) was achieved by partially stripping off the Ru monolayer in the IR cell according to a reproducible procedure (Figure S4). The variation of the CO stripping waves (Figure S4d) as the Ru content changed are similar to those of a Ru-decorated Pt black samples by spontaneous deposition,[14] suggesting Ru island formation. The Ru packing density of the act-Ru/Pt was determined to be about 49% by using surface Pt oxide reduction charge[15] (Figure S5), which is consistent with the EDS measurements (see Section S6 in the Supporting Information for details). Such a surface composition was also highly stable for $E < 0.9$ V (Figure S6).

For the PtRu/C, the as-received sample was first deposited onto a pre-formed ultrathin (ca. 50 nm) Au film deposited onto the triangular Si prism[16] and air-dried completely. It was then activated (act-PtRu/C) by multiple potential cycles in the IR cell (Figure S7). The IR cell was also amenable to

[*] Dr. D.-J. Chen, Prof. Dr. Y. Y. J. Tong
Department of Chemistry, Georgetown University
37th and O Streets, NW, Washington, DC 20057 (USA)
E-mail: yyt@georgetown.edu

[**] This work was supported by a grant from DOD-ARO (66191-CH). The authors thank Prof. Shi-Gang Sun for his support, as the work reported here was a continuation of a project initiated when D.J.C. was an exchange PhD student from Prof. Sun's lab at Xiamen University, China.

Supporting information for this article is available on the WWW under http://dx.doi.org/10.1002/anie.201503917.

electrolyte exchange under potential control, that is, flow-cell operation between a 0.1 M $HClO_4$ and 0.1 M $HClO_4$ + 0.5 M MeOH electrolyte (abbreviated as E-clean and E-MeOH respectively, in which E stands for electrolyte).

Figure 1a shows the SEIRAS spectra of the MeOH-generated (at −0.035 V), linearly bound CO (M-CO_L) on the Pt thin film, Ru monolayer and act-Ru/Pt respectively taken at −0.035 V. As it is well-known that sub-monolayer Ru deposited on Pt forms islands,[17] the two bands observed can then be reasonably assigned to CO adsorbed on Pt-like sites (Pt without Ru as next-nearest neighbor, M-CO_L-Pt) and Ru-like sites (Ru without Pt as next-nearest neighbor, M-CO_L-Ru). Highly similar results were observed on the act-PtRu/C (Figure 1b), which renders strong support to the conclusion reached in our previous study[12] that the activation of as-received PtRu/C corresponds to generating segregated surface Pt-like and Ru-like ensembles. Notice that the clearly discernable IR bands of M-CO_L-Pt and M-CO_L-Ru on both act-Ru/Pt and act-PtRu/C afford us unique molecular probes to follow closely how MOR takes place on the activated PtRu surfaces.

In Figure 2, the integrated IR intensities of M-CO_L as a function of electrode potential on the pure Pt thin film (a) and the act-Ru/Pt (b) respectively are presented (see the

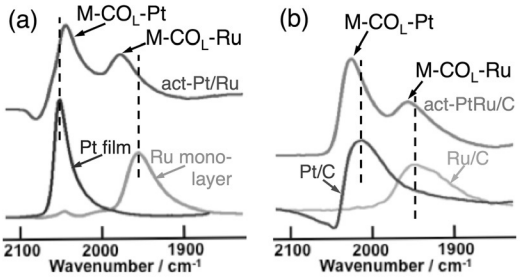

Figure 1. SEIRAS spectra of methanol-generated, linearly adsorbed CO (M-CO_L) at −0.035 V on a) Pt thin film (black), Ru monolayer (light gray), and act-Ru/Pt (dark grsy) and b) Pt/C (black), Ru/C (light gray), and act-PtRu/C (dark gray). The tiny peak at about 2050 cm^{-1} of the Ru monolayer is from CO on very minor amount of pure Pt sites inaccessible to Ru deposition.

Supporting Information, Figure S8 for comparison between the pure J-M Pt/C (40 % wt) and the act-PtRu/C) during MOR in E-MeOH; spectra in Figure S9). Also presented are the associated MOR currents and integrated IR intensities of methanol-generated (adsorbed) formate (M-FM_{abs}). For both the pure Pt film (Figure 2a) and Pt/C (Figure S8a), the onset potential of the MOR current coincides with that of the M-CO_L-Pt oxidation, as indicated by the vertical dashed lines, which is the clear manifestation of the well-known CO poisoning of Pt surface during MOR.[18] For both the act-Ru/Pt (Figure 2b) and act-PtRu/C (Figure S8b), however, differences appear. First, the onset potential of the MOR current (indicated by the vertical arrows) does not coincide with that of the M-CO_L-Pt oxidation (indicated by the vertical dashed lines). The former is at least circa 0.1 V lower than the latter. On the other hand, the onset potential of M-FM_{abs} appears to

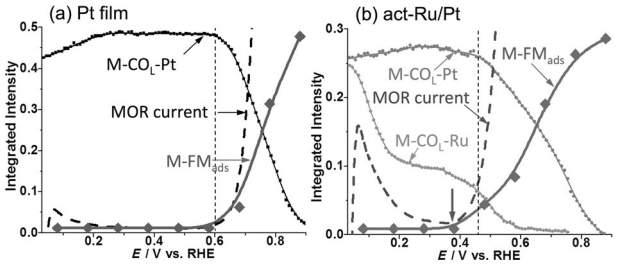

Figure 2. The integrated IR intensity of M-CO (●), MOR current (——), and M-FM_{ads} (◆) as a function of electrode potential during MOR in E-MeOH on a) the pure Pt thin film and b) the act-Ru/Pt, as indicated by the respective arrows. The vertical dashed lines in (a) indicates the coinciding onset potentials of the MOR current and M-CO_L-Pt oxidation but only the onset potential of the latter in (b). The onset potential of the MOR current in (b) is indicated by the vertical arrow pointing towards the bottom axis.

coincide with that of the MOR current. Second, in great contrast to the persistence of the M-CO_L-Pt below 0.465 V (the vertical dashed lines in Figure 2b and Figure S8b), the integrated IR intensity of M-CO_L-Ru decreases very early on.

That the amount of the M-CO_L-Pt during the MOR was almost constant in the potential range lower than 0.5 V in which the enhancement in MOR on both the act-Ru/Pt and act-PtRu/C is already very much operational (Figure 2b; Figure S8b), that is, the enhancement in MOR was not accompanied by the elimination of the adsorbed M-CO_L-Pt, is in clear contradiction to what is expected from Reaction (1). The latter is the basis for the W-M bifunctional mechanism,[9] unless the system reached a dynamic steady-state in which the rate of adsorption of the M-CO_L onto Pt sites equaled to the rate of Reaction (1), as argued previously.[11a]

Two possible reaction pathways could sustain the aforementioned reaction steady-state. The first would involve the CO diffusion from a Pt-like to an adjacent Ru-like site and then be oxidized at the latter site as apparently the M-CO_L-Ru could be eliminated at much lower potential (Figure 2b; Figure S8d). The second would be that the M-CO_L-Pt is oxidized as in Reaction (1) but the freed Pt-like sites are occupied within a time shorter than the IR acquisition by CO diffusion from the neighboring sites or/and by newly adsorbed M-CO from the solution. We carried out two different types of flow-cell based diagnostic experiments to assess whether or not these two possible reaction pathways were operational.

To assess the possible CO diffusion between the Pt- and Ru-like sites, we first populate the surface sites of the act-PtRu/C with saturated M-CO using the flow cell while the uptake of M-CO_L was being measured by SEIRAS (Figure S10a). After replacing the E-MeOH with E-clean, we ran stair-step electrode-potential-dependent SEIRAS measurements as the pre-adsorbed M-CO_L was stripped off (Figure S10b). Since there was no MeOH in the electrolyte as the CO-generating source and the M-CO-Ru could be eliminated at much lower potential than M-CO_L-Pt (Figure 2b), any CO diffusion between the Pt- to Ru-like sites would reduce the IR intensity of the former as the latter being eliminated. The results are shown in Figure 3a and b for the M-CO_L uptake and stripping, respectively. As can be seen, the IR intensity of

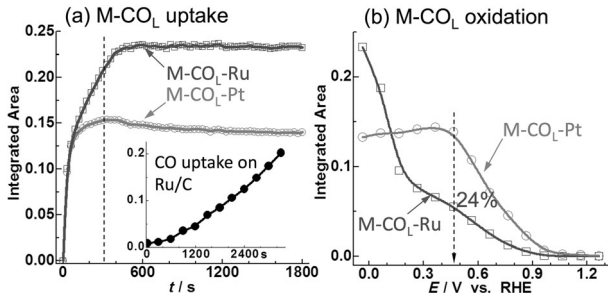

Figure 3. a) The uptake of M-CO$_L$ on the act-PtRu/C at −0.035 V during a flow-cell experiment as measured by integrated IR intensities of the M-CO$_L$-Pt and M-CO$_L$-Ru as indicated by the respective arrows. At $t = 0$, E-MeOH started being flowed into the IR cell to replace the initial E-clean there. The E-MeOH flow continued until 300 s (the vertical dashed line) at which the flow was switched to E-clean that continued up to 1800 s. Time-dependent SEIRAS spectra were recorded over the entire 1800 s. It is interesting to note that the uptake of M-CO$_L$-Ru on act-PtRu/C was much faster than on a pure Ru/C (inset). b) The integrated IR intensities of the M-CO$_L$-Pt and M-CO$_L$-Ru as indicated by the arrows as a function of electrode potential during a stripping of the M-CO$_L$ formed in (a) but in E-clean. At the onset potential of M-CO$_L$-Pt oxidation (the vertical dashed arrow), the amount of M-CO$_L$-Ru remained is only 24% of the initial value.

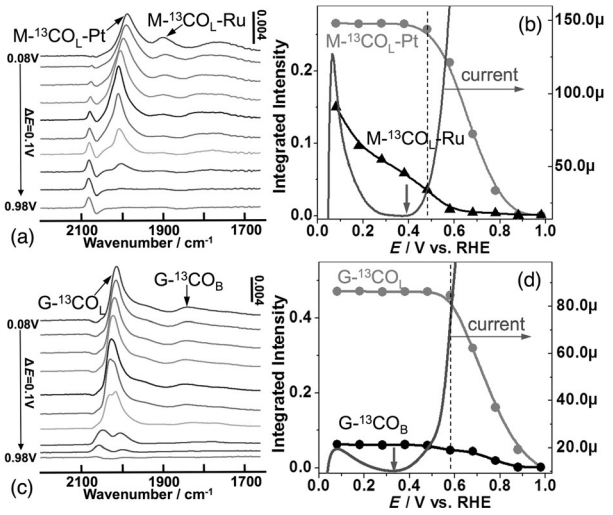

Figure 4. a) SEIRAS spectra of pre-adsorbed M-^{13}CO$_L$ on the act-Ru/Pt as a function of electrode potential in E-MeOH. The tiny peak close to 2100 cm^{-1} is from M-CO$_L$ on minor pure Pt sites inaccessible to Ru deposition. b) The integrated IR intensity of the M-^{13}CO$_L$-Pt (●) and M-^{13}CO$_L$-Ru (▲) as a function of electrode potential. The vertical dashed line indicates the onset potential of M-^{13}CO$_L$ oxidation. The solid curve for the corresponding MOR CV current is indicated by the horizontal arrow and its onset potential by the vertical arrow at about 0.4 V. c), d) Same as (a) and (b) except that the pre-adsorbed ^{13}CO was from ^{13}C-labeled CO gas and the black circles are for the bridge-bound CO.

the M-CO$_L$-Pt remained largely invariant up to about 0.5 V while that of the M-CO$_L$-Ru had a reduction of about 76% (Figure 3b). Furthermore, that the pattern of decrease in the integrated IR band intensity of the M-CO$_L$-Ru in Figure 3b (measured in E-clean) is the same as in Figure 2b (measured in E-MeOH) indicates the same reaction mechanism. We therefore conclude that there was little if any CO diffusion between Pt- and Ru-like sites, which is in agreement with previous NMR studies.[14]

As to whether or not a fast replenishing of M-CO$_L$ to the Pt-like sites freed by Reaction (1) can sustain the hypothetic steady state, we utilized ^{13}C-labeled MeOH and gaseous CO (G-CO) in the following fashion. We first started with the electrocatalyst surface pre-adsorbed with either M-^{12}CO/G-^{12}CO or M-^{13}CO/G-^{13}CO at −0.035 V then ran MOR cyclic voltammetry (CV) in ^{13}C-labeled E-MOH for the former or normal E-MeOH for the latter respectively. If the fast CO replenishing hypothesis were correct, it would be observed that the pre-adsorbed M-CO/G-CO be replaced by M-CO of a different carbon isotope, which is discernible by in situ SEIRAS. Figure 4 presents the case with M-^{13}CO/G-^{13}CO on the act-Ru/Pt: (a),(c) shows the SEIRAS spectra and (b),(d) the corresponding integrated IR intensities as a function of electrode potential during the MOR CV whose current is presented in (b),(d), respectively. We note that no CO_2 band was observed here owing to fast diffusion of the reaction-generated CO_2 away from the open surface structure of the Ru/Pt thin film, which is in contrast to the act-PtRu/C (Figure S11). The microporous structure of the deposited PtRu/C can retain reaction-generated CO_2 much longer so its IR band becomes observable. We also note that for still unknown reason, the gaseous CO adsorption on either the act-Ru/Pt or the act-PtRu/C does not generate a clear IR band assignable to the CO$_L$ on Ru-like sites. However, its absence does not have any bearings on the conclusions of this work. Since M-^{12}CO has higher vibration frequency than the M-^{13}CO/G-^{13}CO, even a small amount of M-^{12}CO on the surface would be amplified by the IR intensity transfer from the low-frequency M-^{13}CO/G-^{13}CO to the high-frequency M-^{12}CO if they indeed coexist on the surface.[19] As can be seen, a clearly discernable M-^{12}CO IR band does not appear until about 0.68 V (Figure 4a,c), while the onset of MOR already started at about 0.39 V/0.33 V (the vertical arrows in Figure 4b,d). The constant integrated IR intensity of the M-^{13}CO/G-^{13}CO below 0.5 V where the MOR was already operational (Figure 4b,d) indicates strongly that neither the M-^{13}CO nor the G-^{13}CO was replenished by M-^{12}CO as expected by Reaction (1). Similar results were also obtained on the act-PtRu/C (Figure S11).

It becomes now convincingly clear from the above observations that Reaction (1), that is, the kernel of the W-M bifunctional mechanism, proposed some four decades ago and has been widely accepted as the prevailing guiding theorem for designing and developing CO-poisoning-tolerant bimetallic electrocatalysts for DMFCs, is not an adequate mechanism for the enhanced MOR observed on both the act-Ru/Pt and act-PtRu/C electrocatalysts at the low overpotential. That is, the so-called CO poisoning of the Pt-like sites is largely irrelevant for the enhanced MOR on the activated PtRu surface. Now the intriguing question is what the right mechanism is.

That 1) no M-^{12}CO was generated during the MOR with the pre-adsorbed M-^{13}CO/G-^{13}CO (Figure 4) or vice versa (Figure S11) and 2) the pre-adsorbed G-CO could not block the active sites responsible for the enhanced MOR observed either on the act-Ru/Pt (Figure 4c,d) or act-PtRu/C (Fig-

ure S11 c,d) suggests strongly that the enhanced MOR follows a reaction pathway that does not lead to the generation of M-CO, like CN-modified Pt(111),[5e] which implies strongly that it followed the direct reaction pathway in which formate is expected to be a reaction intermediate.[5c,d] Indeed, M-FM_{ads} at potentials below 0.5 V was only observed on the act-Ru/Pt but none on the pure Pt film (Figure S12).

As alluded in Figure 1, we have recently shown that the activation procedure leading to the act-PtRu/C causes a dynamic re-distribution of the surface Pt and Ru sites that leads to more segregated distributions of each element.[12] It is highly likely that the best activation corresponds to an approximately equal amount of segregated surface Pt-like and Ru-like ensembles that maximizes the Pt-Ru boundaries (that is, PtRu sites that have the other element as at least one of the next-nearest neighbors).[12] With this in mind, we propose the following revised bifunctional mechanism responsible for the enhanced MOR on both the act-Ru/Pt and act-PtRu/C electrocatalyst (and PtRu electrocatalysts in general):

$$Ru^* + H_2O \rightarrow Ru{-}OH + H^+ + e^- \quad (2a)$$

$$PtRu^* + CH_3OH \rightarrow PtRu{-}OCH_3 + H^+ + e^- \quad (2b)$$

$$PtRu{-}OCH_3 + Ru{-}OH \rightarrow PtRu{=}OOCH + Ru^* + 3(H^+ + e^-) \quad (2c)$$

$$PtRu{=}OOCH \rightarrow PtRu^* + CO_2 + H^+ + e^- \quad (2d)$$

where Ru* and PtRu* stand for the unoccupied Ru-like and PtRu sites (Pt-like sites are occupied by M-CO during MOR at potentials below 0.5 V; see Figure 2 b and Figure S8 b) and =OOCH represents bidentate formate. Note that the proposed reaction mechanism requires that the free Ru* and PtRu* sites must be next to each other and available, a surface configuration that is maximized by the activation process.[12]

Among the proposed four reaction steps in Reaction (2), step (2a) is expected to be a facile one.[20] Evidence (Figure S13) suggests that the initial fast decrease in the M-CO_L-Ru IR band intensity was highly likely due to a displacement of the M-CO_L-Ru by the OH adsorption in step (2a). To assess step (2d), we carried out another type of flow cell measurements on the act-Ru/Pt as follows. We first ran a CA of MOR in E-MeOH at 0.465 V for 300 s as shown by the light-gray curve in Figure 5 a, then carried out an exchange of electrolyte with 0.5 M formic acid (E-FA) at −0.035 V, and finally ran a CA of FA oxidation reaction (FAOR) at 0.465 V for another 300 s as shown by the dark curve in Figure 5 a after completing the exchange of electrolyte. What we observed is that the FAOR current at 300 s was 6 times (12 times were obtained on the PtRu/C supported on glassy carbon; Figure S14) higher than that of the MOR. As shown in the inset of Figure 5 a, higher FAOR current went with the higher IR band intensity of the M-FM_{ads}. As the Pt-like sites were occupied by M-CO, the much higher FAOR current shown in Figure 5 a suggests strongly that step (2d) should be much faster than step (2c). However, the latter is the key step of the revised bifunctional MOR mechanism.

While step (2b) is expected for the direct MOR pathway[5d] and can become the dominant pathway because all

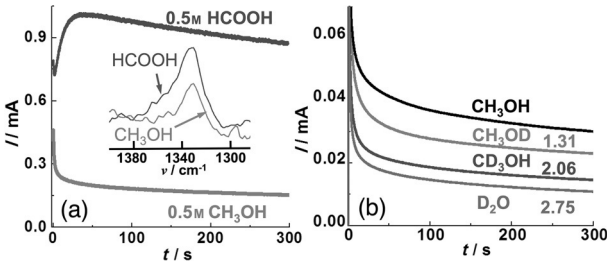

Figure 5. a) The CA curves at 0.465 V of MOR (light) and FAOR (dark) on the same act-Ru/Ru recorded using flow cell (see the text for details). The FAOR current at 300 s is about 6 times (12 times on the act-PtRu/C) higher than that of MOR. Inset: the respective IR band of M-FM_{ads}. b) The kinetic isotope effect (KIE) of MOR at 0.465 V measured on an act-PtRu/C deposited on a glassy carbon electrode. The numbers are the corresponding KIEs.

available Pt-like sites are now occupied by M-CO, little is known about how MeOH would interact with the PtRu* sites. What we do know are that 1) the dissociation of MeOH to CO on pure Ru is very slow (inset in Figure 3 a and Figure S13) but M-CO can be generated on the Ru-like sites of a PtRu surface as quick as on the Pt-like sites (Figure 3 a); and 2) there is no CO diffusion between Pt- and Ru-like sites (Figure 3 b). If we assume that the Ru-like sites would behave more like pure Ru, then the fast-generated M-CO_L-Ru could only come from the PtRu sites with C and O of the approaching MeOH favoring the Ru and Pt, respectively, because the M-CO so generated would have C bound to Ru and could diffuse easily to adjacent Ru-like sites. That the M-CO_L-Ru was the dominant adsorbate on the surface of the as-received PtRu/C (Figure S15) supports the C-down-to-Ru conjecture. Moreover, such an interaction configuration would also facilitate the oxygen insertion in step (2c) and its selectivity would become higher under reaction condition in which the Pt-like sites are largely occupied by M-CO.

To further assess the proposed MOR mechanism in Reaction (2), we also studied the kinetic isotope effect (KIE)[21] of MOR on the act-PtRu/C as presented in Figure 5 b. When CH_3OH was replaced by CH_3OD or CD_3OH, or H_2O by D_2O, the KIE $= K_H/K_D = I_H/I_K = 1.3$, 2.1, or 2.8, respectively, was observed. That is, D_2O had the largest KIE. Among the four steps in Reaction (2), only steps (2a) and (2c) involves the species from D_2O. As step (2a) is facile, we identify (2c), particularly the breaking of O–H bond in Ru–OH, as the rate-limiting step for MOR on the activated PtRu/C. Further experimental support of this come from the data shown in Figure 6 a and 6 b, where the MOR activity is measured as a function of $H_2O/(H_2O + D_2O)$ ratio and of pH value in alkaline environment respectively (see the Supporting Information, Figure S16 for details).

Specifically, when H_2O is mixed with D_2O at a low percentage, H_2O will all become HDO owing to fast H and D exchange. As O–H is easier than O–D to break due to the KIE, this will lead to only Ru–OD despite the presence of H_2O, which explains why the MOR activity did not increase when the H_2O percentage was lower than 20 % (Figure 6 a). Once water can exist in the form of H_2O as its content increases, Ru–OH will form, which leads to a linear increase

in MOR activity as observed in Figure 6a. Moreover, when MOR CVs were run in NaOH solution as a function of pH, the current peak potential did not change (Figure S16b), indicating that the same reaction mechanism was operational for all pH values. However, the peak current did show a volcano shape as shown in Figure 6b. This can be understood as follows. As the pH increases, more Ru–OH is formed, which facilitates reaction step (2c), so increasing the reaction current. But a further increase in pH leads to a surface poisoned by excessive OH, thus decreasing the reaction current. The results of the both measurements are consistent with the proposed MOR reaction mechanism as shown by the representation in Figure 6c.

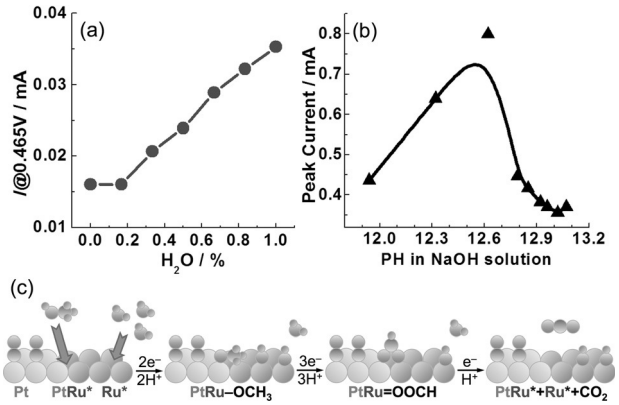

Figure 6. a) The CA currents at 300 s recorded at 0.465 V on the act-PtRu/C as a function of H_2O percentage content in a mixed H_2O and D_2O. b) The MOR CV peak current on the act-PtRu/C in a NaOH electrolyte as a function of pH value. c) Representation of the proposed MOR reaction mechanism on the act-PtRu/C.

In summary, by combining in situ SEIRAS with the unique experimental control offered by flow cell operations and diagnostic selectivity by isotope labeling, we have shown that the long-believed poisonous CO on the Pt sites of a PtRu surface was not part of the reactions that led to the enhanced MOR activity on the latter as observed and therefore Reaction (1) is irrelevant to enhancing MOR at low overpotential (< 0.5 V). We have proposed a revised bifuntional mechanism, Reaction (2), accordingly, which is consistent with data presented in Figures 5 and 6. We expect that the conclusion reached herein should be robust and general as it came from consistent results obtained on two very different PtRu systems. Consequently, it will have broad implications, stimulate further research, and help design better MOR catalysts for DMFC applications.

Keywords: ATR-SEIRAS · CO poisoning · methanol oxidation reaction · PtRu electrocatalysis · reaction mechanisms

How to cite: *Angew. Chem. Int. Ed.* **2015**, *54*, 9394–9398
Angew. Chem. **2015**, *127*, 9526–9530

[1] R. Parsons, T. VanderNoot, *J. Electroanal. Chem.* **1988**, *257*, 9–45.
[2] G. A. Olah, *Angew. Chem. Int. Ed.* **2013**, *52*, 104–107; *Angew. Chem.* **2013**, *125*, 112–116.
[3] B. C. H. Steele, A. Heinzel, *Nature* **2001**, *414*, 345–352.
[4] a) W. Vielstich, X. H. Xia, *J. Phys. Chem.* **1995**, *99*, 10421–10422; b) E. Herrero, W. Chrzanowski, A. Wieckowski, *J. Phys. Chem.* **1995**, *99*, 10423–10424; c) E. Herrero, K. Franaszczuk, A. Wieckowski, *J. Phys. Chem.* **1994**, *98*, 5074–5083.
[5] a) T. Iwasita, *Electrochim. Acta* **2002**, *47*, 3663–3674; b) T. D. Jarvi, S. Sriramulu, E. M. Stuve, *J. Phys. Chem. B* **1997**, *101*, 3649–3652; c) Y. X. Chen, A. Miki, S. Ye, H. Sakai, M. Osawa, *J. Am. Chem. Soc.* **2003**, *125*, 3680–3681; d) T. H. M. Housmans, A. H. Wonders, M. T. M. Koper, *J. Phys. Chem. B* **2006**, *110*, 10021–10031; e) A. Cuesta, *J. Am. Chem. Soc.* **2006**, *128*, 13332–13333.
[6] A. S. Arico, V. Baglio, V. Antonucci, in *Electrocatalysis of Direct Methanol Fuel Cells* (Eds.: H. Liu, J. Zhang), Wiley-VCH, Weinheim, **2009**, pp. 1–78.
[7] O. A. Petrii, *J. Solid State Electrochem.* **2008**, *12*, 609–642.
[8] M. Watanabe, S. Motoo, *J. Electroanal. Chem.* **1975**, *60*, 267–273.
[9] T. Yajima, H. Uchida, M. Watanabe, *J. Phys. Chem. B* **2004**, *108*, 2654–2659.
[10] H. A. Gasteiger, N. Markovic, P. N. Ross, E. J. Cairns, *J. Phys. Chem.* **1993**, *97*, 12020–12029.
[11] a) T. Iwasita, H. Hoster, A. John-Anacker, W. F. Lin, W. Vielstich, *Langmuir* **2000**, *16*, 522–529; b) D. Kardash, C. Korzeniewski, N. Markovic, *J. Electroanal. Chem.* **2001**, *500*, 518–523.
[12] D. J. Chen, S. G. Sun, Y. Y. J. Tong, *Chem. Commun.* **2014**, *50*, 12963–12965.
[13] a) A. Miki, S. Ye, M. Osawa, *Chem. Commun.* **2002**, 1500–1501; b) M. Watanabe, T. Sato, K. Kunimatsu, H. Uchida, *Electrochim. Acta* **2008**, *53*, 6928–6937; c) D. J. Chen, A. M. Hofstead-Duffy, I. S. Park, D. O. Atienza, C. Susut, S. G. Sun, Y. Y. J. Tong, *J. Phys. Chem. C* **2011**, *115*, 8735–8743.
[14] Y. Y. Tong, H. S. Kim, P. K. Babu, P. Waszczuk, A. Wieckowski, E. Oldfield, *J. Am. Chem. Soc.* **2002**, *124*, 468–473.
[15] B. Du, S. A. Rabb, C. Zangmeister, Y. Y. Tong, *Phys. Chem. Chem. Phys.* **2009**, *11*, 8231–8239.
[16] D.-J. Chen, B. Xu, S.-G. Sun, Y. Y. J. Tong, *Catal. Today* **2012**, *182*, 46–53.
[17] E. Herrero, J. M. Feliu, A. Wieckowski, *Langmuir* **1999**, *15*, 4944–4948.
[18] a) G. A. Camara, E. A. Ticianelli, S. Mukerjee, S. J. Lee, J. McBreen, *J. Electrochem. Soc.* **2002**, *149*, A748; b) Q. Li, R. He, J.-A. Gao, J. O. Jensen, N. J. Bjerrum, *J. Electrochem. Soc.* **2003**, *150*, A1599.
[19] a) C. S. Kim, W. J. Tornquist, C. Korzeniewski, *J. Chem. Phys.* **1994**, *101*, 9113–9121; b) J. A. Rodriguez, C. M. Truong, D. W. Goodman, *J. Chem. Phys.* **1992**, *96*, 7814–7825.
[20] S. Hadzi-Jordanov, H. Angerstein-Kozlowska, M. Vukovic, B. E. Conway, *J. Phys. Chem.* **1977**, *81*, 2271–2279.
[21] a) J. Bigeleisen, M. Wolfsberg, in *Adv. Chem. Phys., Vol. 1* (Eds.: I. Prigogine, P. Debye), Wiley, New York, **1958**, pp. 15–76; b) F. H. Westheimer, *Chem. Rev.* **1961**, *61*, 265–273.

Received: April 29, 2015
Published online: July 6, 2015

